

Observational Appearance of Relativistic, Spherically Symmetric Massive Winds

Naoko SUMITOMO, Shinji NISHIYAMA, Chizuru AKIZUKI *, Ken-ya WATARAI †, Jun FUKUE
Astronomical Institute, Osaka Kyoiku University, Asahigaoka, Kashiwara, Osaka 582-8582
j069338@ex.osaka-kyoiku.ac.jp, fukue@cc.osaka-kyoiku.ac.jp

(Received 2006 0; accepted 2006 0)

Abstract

The photon mean free path in a relativistically moving medium becomes long in the down-stream direction while short in the up-stream direction. As a result, the observed optical depth τ becomes small in the downstream direction while large in the upstream direction. Hence, if a relativistic spherical wind blows off, the optical depth depends strongly on its speed and the angle between the velocity and the line-of-sight. Abramowicz et al. (1991) examined such a relativistic wind, and found that the shape of the photosphere at $\tau = 1$ appears convex in the non-relativistic case, but concave for relativistic velocities. We further calculated the temperature distribution and luminosity of the photosphere both in the comoving and inertial frames. We found that the limb-darkening effect would strongly modified in the relativistic regime. We also found that luminosities of the photosphere becomes large as the wind speed increases due to the relativistic effects. In addition, the luminosity in the inertial frame is higher than that in the comoving frame. These results suggest that the observed temperature and brightness in luminous objects may be overestimated when there are strong relativistic winds.

Key words: accretion disks — black hole physics — radiative transfer — relativity — winds

1. Introduction

Recent observations have revealed the existence of highly luminous objects, such as ultraluminous X-ray sources (ULXs) in nearby galaxies, narrow line Seyfert 1 galaxies (NLS1s), and bright PG quasars. Bright objects are paid to attention because the outflow is observed in those objects. Quasar PG 1211+143 seems to have relatively high velocity outflow ($v \sim 0.1c$) from their broad absorption line features observed by *XMM-Newton* (Pounds et al. 2003a). Quasar PG 0844+349 also shows several absorption features in its X-ray spectrum, and the outflow velocity is on the order of $\sim 0.2c$ (Pounds et al. 2003b). Moreover, PKS 1549-79 is a luminous quasar-like active galactic nucleus, and contains relatively narrow permitted lines, highly blue-shifted [O III] lines, which are well-observed in NLS1s. The Very Large Telescope (VLT) observation of PKS 1549-79 shows outflow-like images, thus there is evidence that high mass accretion and warm outflow coexist in this object (Holt et al. 2006).

Optical observations of broad absorption line (BAL) quasars also suggested the existence of not-collimated, relativistic outflows. Typical wind velocity estimated by their line width is about $10000\text{--}30000 \text{ km s}^{-1}$. The high column density of $N_{\text{H}} \sim 10^{23\text{--}24} \text{ cm}^{-2}$ suggests that large amounts of gas are moving around the central region of BAL quasars.

King and Pounds (2003) recently suggested that highly optically thick, relativistic winds — “black hole winds” — blow off from the central part of accretion disks, and produce a large luminosity, which may be observed in quasar PG 1211+143 and ULXs. If the mass-outflow rate of the wind increases, the optical depth of the wind exceeds unity, and eventually such a massive wind may form a “photosphere” like the sun. The location of the photosphere depends on the wind velocity and mass-outflow rate, then we may observe the light from an outflow rather than that from an accretion disk. Therefore, the determination of the location of the photosphere is quite important from the observational viewpoint.

Spherically symmetric, relativistic winds have been investigated by several researchers (e.g., Castor 1972; Ruggles, Bath 1979; Mihalas 1980; Quinn, Paczyński 1985; Turolla et al. 1986; Paczyński 1990; Akizuki, Fukue 2007), and their models have applied to neutron star winds and gamma-ray burst (GRB). However, in these studies they focused on the dynamics of the relativistic outflow, and not concentrated on the observational implications. Abramowicz et al. (1991) first examined the observational appearance of the relativistic, spherical winds, using a simple model at a constant speed. They found that the shape of the photosphere appears convex in the non-relativistic case, but concave in a relativistic regime.

* Present address: Center for Computational Physics, University of Tsukuba, Tennoudai 1-1-1, Tsukuba, Ibaraki, 305-8577

† Research Fellow of the Japan Society for the Promotion of Science

Abramowicz et al. (1991) only considered the apparent shape of the photosphere of the relativistic spherical winds. Thus, in this paper, we further examine the relativistic spherical winds, focusing our attention to the observational appearance, such as an observed temperature distribution and an emergent luminosity, and give observational implications to several PG quasars and ULXs.

In section 2, we briefly introduce the present wind model, and describe the calculation method. Section 3 demonstrates the results, and the discussions and applications are presented in section 4. Final section is devoted to concluding remarks.

2. Model and Calculation Method

In this section we describe the present wind model and calculation method.

2.1. Wind Model

Our present model is based on the model by Abramowicz et al. (1991). We briefly summarize the simple model at a constant velocity.

We assume that a spherically symmetric, relativistic wind blows off from a central object. As a central object, we assume a non-rotating black hole (Schwarzschild black hole), and the Schwarzschild radius is defined by $r_g = 2GM/c^2$, where G , M , and c represent the gravitational constant, black hole mass, and the speed of light, respectively. We use the spherical coordinates (R, θ, φ) and the cylindrical coordinate (r, φ, z) , whose z -axis is along the line-of-sight (see figure 1).

From continuity equation, the rest mass density ρ_0 measured in the comoving frame varies as

$$\rho_0 = \left(\frac{\dot{M}}{4\pi v \gamma} \right) R^{-2}, \quad (1)$$

where \dot{M} is the mass-loss rate, $R = \sqrt{r^2 + z^2}$ is a distance from the central object, and γ is the Lorentz factor of the wind expressed as

$$\gamma \equiv (1 - \beta^2)^{-1/2}, \quad \beta \equiv \frac{v}{c}. \quad (2)$$

Quantities with subscript “0” refer to physical quantities measured in the comoving frame.

In the present simple model, the mass-loss rate \dot{M} and wind velocity v are assumed to be constant.

2.2. Photosphere of the Wind

We define an “apparent photosphere” of the wind as the surface, where the optical depth τ measured from an observer becomes unity. Schematic picture of our present calculation is presented in figure 1.

Lets us consider a small distance ds along the light path. Due to the relativistic effect, the mean free path of photons in the fixed frame, ℓ , is related to that in the comoving frame, ℓ_0 , by

$$\ell = \frac{1}{\gamma(1 - \beta \cos\theta)} \ell_0, \quad (3)$$

where θ is the viewing angle measured from the z -axis. Then, the optical depth in the fixed frame is given by

$$d\tau = \gamma(1 - \beta \cos\theta) \kappa \rho_0 ds, \quad (4)$$

where the opacity κ is assumed to be electron scattering (Abramowicz et al. 1991). Thus, the optical depth strongly depends on the viewing angle θ as well as the flow speed v . It is obvious that the optical depth is smallest in the downstream direction at $\theta = 0$, where the photons move in the same direction with the fluid, while it becomes largest in the upstream direction at $\theta = \pi$, where the photons move in the opposite direction to the fluid.

From equation (4), the integrated optical depth τ_{ph} from an observer at infinity is calculated as

$$\tau_{\text{ph}} = \int_{z_{\text{ph}}}^{\infty} \gamma(1 - \beta \cos\theta) \kappa \rho_0 ds = 1, \quad (5)$$

where z_{ph} is location of the apparent photosphere from the equatorial plane. Abramowicz et al. (1991) showed that the photosphere of a highly relativistic wind is much closer to the source, roughly by a factor γ^2 . Although the non-relativistic and moderately relativistic winds have convex photospheres, the photospheres of relativistic wind becomes concave for $\beta > 2/3$ (see figure 2).

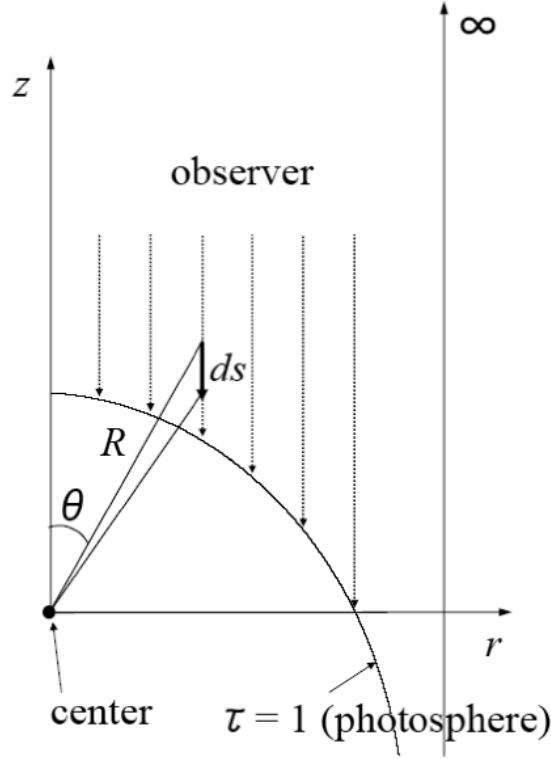


Fig. 1. Schematic picture of the present calculation. The spherical wind is assumed to blow off from the origin at a relativistic speed. The observer is located at infinity in the z -direction.

2.3. Temperature Distribution and Luminosity

In the present model, we assume that the spherical wind expands adiabatically. Then, the temperature T_0 of the wind gas in the comoving frame varies as $T_0 \propto \rho_0^{\Gamma-1} \propto \rho_0^{1/3} \propto R^{-2/3}$, where Γ is the ratio of specific heats, and set to be $4/3$ for a radiation pressure dominant regime. Hence, the temperature distribution in the comoving frame is

$$\frac{T_0}{T_c} = \left(\frac{R}{R_c} \right)^{-2/3}, \quad (6)$$

where T_c is the central temperature at $R = R_c$.

Furthermore, the observed temperature T in the observer's frame is expressed by

$$T = \frac{1}{1+z} T_0 = \frac{1}{\gamma(1-\beta \cos \theta)} T_0, \quad (7)$$

where z is the redshift via longitudinal and transverse Doppler effects. Using this observed temperature, we can obtain the observed luminosity by

$$L = \int_{r_{\text{in}}}^{r_{\text{out}}} 2\pi r dr \times F dr, \quad (8)$$

where F is the observed flux, $F = \sigma T^4$ when we assume the blackbody radiation, σ being the Stefan-Boltzmann constant. This integration has been performed at $z \rightarrow \infty$ in the observer's frame, thus the effect of curvature of the photosphere is automatically included.

3. Results

We determined the photosphere for various β via equation (5), and obtained the temperature and luminosity on the surface of the photosphere in the comoving and inertial frames. In the present calculation, we bear in mind the case for active galactic nuclei, although the present results are also important for black-hole binaries. Hence, the black hole mass and temperature at the central region are fixed as $M = 10^7 M_\odot$ and $T_c = 10^7 K$, respectively. The

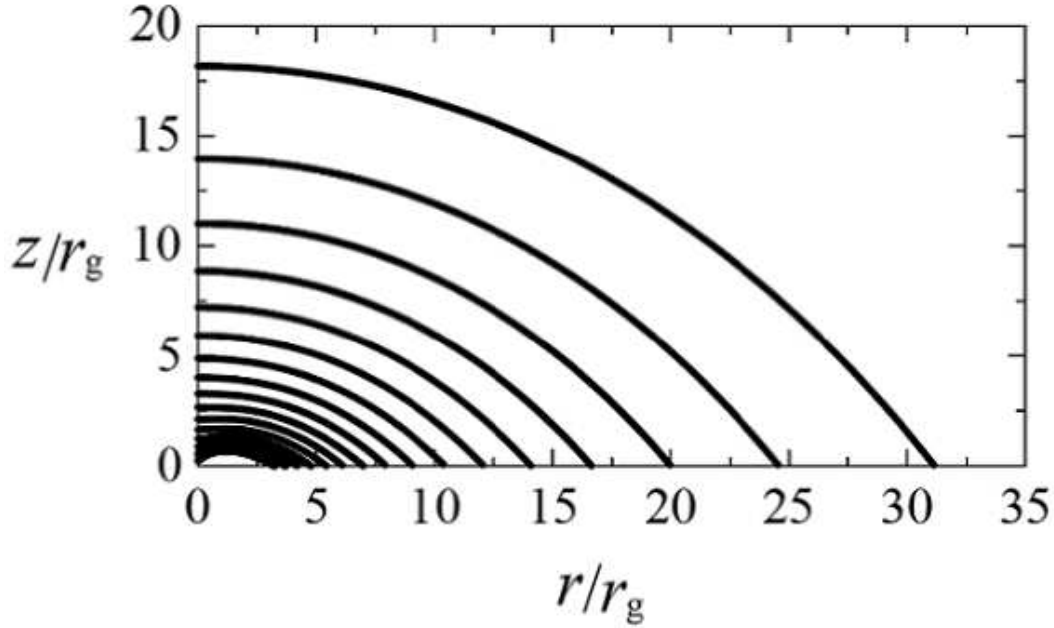


Fig. 2. Location of the photosphere for various wind velocity β . The wind velocity is varied from 0.95 (central region) to 0.20 (outer region) in steps of 0.05. The units of the r - and z -axis is the Schwarzschild radius r_g .

input parameters are then the velocity β and the normalized mass-loss rate \dot{m} of wind, where the mass-loss rate is normalized by the critical rate, $\dot{m} = \dot{M}/\dot{M}_{\text{crit}} = \dot{M}/(L_E/c^2)$, L_E being the Eddington luminosity.

3.1. Location of the Photosphere

Figure 2 shows the location of the apparent photosphere seen by the observer at infinity in the z -direction for various wind velocities. In the low speed regime, the photosphere near the z axis is close to the center, while the photosphere far away from the z axis is far from the center. This is the usual limb-darkening effect of the spherically expanding wind.

In the high speed regime, on the other hand, the shape of the apparent photosphere changes, because the optical depth depends on the angle θ and the wind velocity v . In particular, when the wind blows off at highly relativistic speed ($\beta \geq 0.8$), the photosphere looks like a concave shape.

Our results consistent with the analytical results by Abramowicz et al. (1991), but we note that the units of our coordinate is the Schwarzschild radius r_g .

3.2. Temperature Distribution

In figure 3 we show the temperature distributions in the comoving and inertial frames, respectively, viewed by an observer at infinity in the direction of the z -axis. In general, the wind photosphere looks brightest at the central part, and the surroundings are gradually dim as increasing radius. This is due to the limb darkening effect seen in the usual spherical wind.

In the relativistic wind considered here, however, this limb-darkening effect is remarkably enhanced. This is due in part to the relativistic Doppler and aberration effects, and due in part to the fact that the observed photosphere shrinks as the velocity increases and we can see deep inside the wind.

Comparing the temperature distributions in the comoving and inertial frames, we see that the central temperature in the inertial frame is higher than that in the comoving frame. This is just the relativistic Doppler and aberration effects. That is, the observed temperature increases as θ approaches zero because of the longitudinal Doppler effect (highly beamed emission). This effect also becomes remarkable as the velocity increases.

3.3. Apparent Luminosity

In figure 4 we show the luminosities of the relativistic winds as a function of the wind velocity β for several mass-loss rates \dot{m} . Solid curves represent the observed luminosity in the inertial frame, and the dashed curves show the comoving luminosity.

As is seen in figure 4, the wind luminosity increases as the velocity increases, while it decreases as the mass-loss rate increases. In addition, the luminosity observed in the inertial frame is higher than that in the comoving frame.

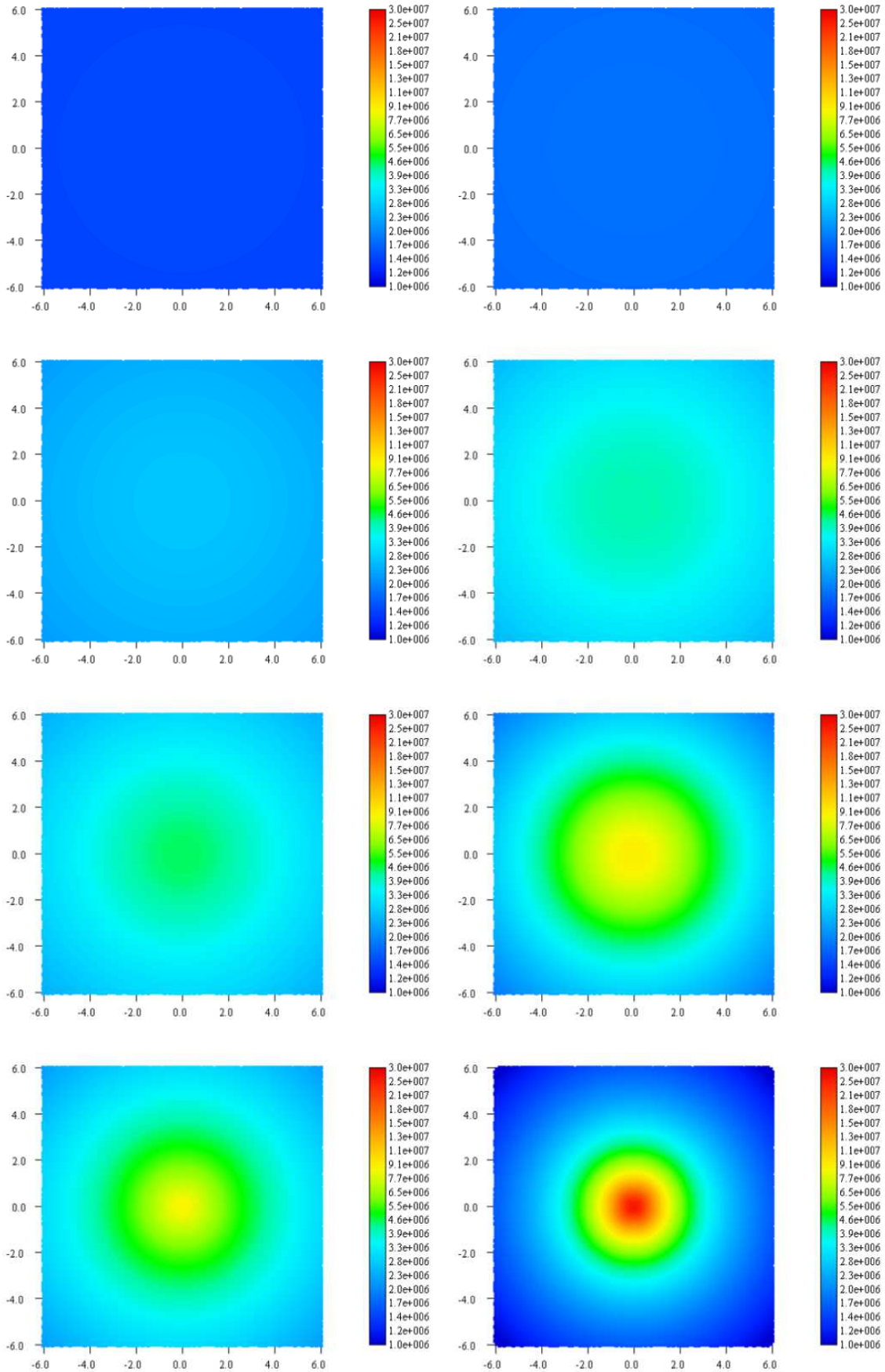


Fig. 3. Temperature distribution at the apparent photosphere viewed by an observer at infinity in the z -direction. The left and right panels show the temperatures in the comoving and fixed (observer's) frames, respectively. The wind velocity β is varied as 0.2, 0.4, 0.6, and 0.8 from top to bottom in both panels.

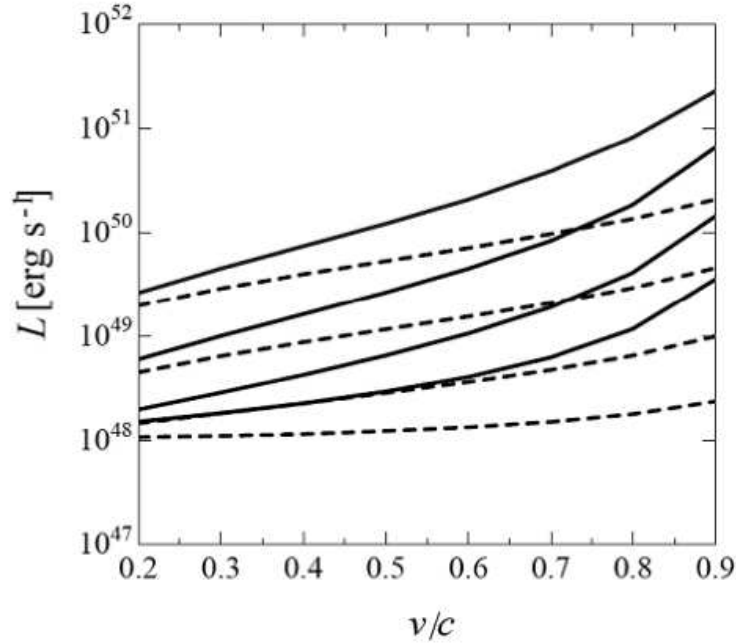


Fig. 4. Luminosity of the relativistic wind as a function of the wind velocity for several mass-loss rates. Solid curves represent the observed luminosity in the inertial frame, and the dashed curves show the comoving luminosity. The mass-loss rate \dot{m} are 10, 100, 1000, and 10000 from top to bottom.

In the present calculation, the location of the photosphere strongly depends on the density of the wind. Namely, as the mass-loss rate increases, the wind density increases, and the location of the photosphere expands to the outer region. Since the temperature of the wind in the outer region is lower than that in the inner region, the luminosity decreases as the mass-loss rate increases.

Moreover, by the effect of Doppler beaming, the observed luminosity increases as the velocity increases. It is emphasized that the comoving luminosity is enhanced about 130 percent for $\beta = 0.2$, but the amplification is about one order for $\beta = 0.9$. These facts suggest that there is a possibility of overestimation of the observed luminosities for relativistic outflow objects.

4. Discussions

4.1. Observational Importance of the Apparent Photosphere

The observed shape of the photosphere is asymmetric in spite of spherically symmetric winds. This is due to the limb-darkening effect. This nature does not depend on the observer's direction. Due to the optical depth effect, we could see deeper inside the wind, as the velocity increases. In addition, the luminosity in the observer's frame is remarkably enhanced by relativistic beaming effects along the observer's direction. These two effects mainly work as the luminosity enhancement of the relativistic outflow.

This fact shows the possibility of overestimation of the temperature and the luminosity of the object that is supposed for wind to blow off at a relativistic speed. When the wind velocity is fast or the mass-loss rate is small, the radius on a bright photosphere becomes small, and we observe higher temperature and higher luminosity. The radius on a bright photosphere increases, when the speed is small or the mass-loss rate increase.

If the wind blows off from the luminous accretion disk surrounding the central object, the disk is concealed by the massive wind, there is a possibility of observing not disk but wind (cf. Nishiyama et al. 2007). There is possibility that the estimate of luminosity and black hole mass different from those actual values.

4.2. Relation to BAL, PG Quasars

The quasar PG 1211+143 is a strong candidate having an optically thick wind driven by radiation pressure, and its wind velocity is roughly estimated to be $0.1c$, using X-ray observation by *XMM-Newton* (Pounds et al. 2003a). Typical velocity of the outflow in BAL quasars also shows sub-relativistic velocities ($\sim 0.1 - 0.3c$). These luminous quasars are likely to have sub-relativistic outflow, thus acceleration mechanism of the wind may be same. It is known that the radiation-pressure driven wind is difficult to be accelerated to highly relativistic speed ($\beta \sim 0.9$), but possible

to be accelerated up to mildly relativistic speed ($\beta \sim 0.1 - 0.3$) (e.g., Icke 1980; Tajima, Fukue 1997; Watarai, Fukue 1999). Recent 2D radiation hydrodynamical simulations also showed massive, optically thick winds from a luminous accretion flow, but their wind velocities are still subrelativistic of $0.1 - 0.3c$ (e.g., Proga 2003; Ohsuga et al. 2005). Unfortunately, a sample number of PG quasars is insufficient for a statistical argument. Moreover, absorption lines observed in PG 0844+349 are highly suspectable because re-analysis of the same data by other group did not confirm the earlier results (Brinkman et al. 2006). Thus we hope further reliable detections of the broad absorption lines in BAL quasars to confirm the existence of mildly relativistic outflows.

5. Concluding Remarks

In this paper, we examined the appearance of relativistic, spherically symmetric wind from the observational point of view. As for the shape of the apparent photosphere of massive winds, we confirmed the results of Abramowicz et al. (1991). We further calculated the temperature distribution and luminosity of the photosphere both in the comoving and inertial frames. We found that the limb-darkening effect would strongly modified in the relativistic regime. We also found that luminosities of the photosphere becomes large as the wind speed increases due to the relativistic effects. In addition, the luminosity in the inertial frame is higher than that in the comoving frame. In particular, the luminosity in the observer's frame is one order of magnitude higher than that in the comoving frame for highly relativistic regimes. We suggest that if the observed luminosity is used for the evaluation of the black hole mass, then the derived black hole mass will be overestimated.

In order to compare with observational data, we need more strict treatments of a wind model, e.g., the effect of general relativity, radiative energy loss in the wind, compton processes, acceleration by radiation pressure, etc. However, the aim of this paper is to show the possibility of the formation of the photosphere. Here, we explicitly show the formation of the photosphere in an optically thick wind using a simple spherical wind model.

Strictly speaking, the observed temperature should be evaluated from the temperature on the surface, where the effective optical depth equals to unity, $\tau_{\text{eff}} = \sqrt{\tau_{\text{ff}} \tau_{\text{tot}}} = \sqrt{\tau_{\text{ff}}(\tau_{\text{ff}} + \tau_{\text{es}})} = 1$, τ_{ff} and τ_{es} being the free-free and electron scattering opacities, respectively. In a high temperature plasma, the effective optical depth is often smaller than the total optical depth, and the gas becomes scattering dominant. In such a scattering dominated plasma, the emergent spectrum is not a simple blackbody but a modified blackbody (e.g., Rybicki and Lightman 1979). In addition, we have used the Thomson cross section for electron scattering. When the center-of-mass energy of scattering becomes relativistic ($h\nu \sim 100$ keV), we should use the Klein-Nishina cross section, which reduces the effective cross section. In such a highly relativistic regime, a wind will be much more transparent. These effects are also left as future problems.

This work was supported in part by the Grant-in-Aid for JSPS fellows (16004706 KW) and for Scientific Research of the Ministry of Education, Culture, Sports, Science, and Technology (18540240 JF).

References

- Abramowicz, M.A., Novikov, I.D., & Paczyński, B., 1991, ApJ, 369, 175
 Akizuki, C., & Fukue, J. 2007, submitted to PASJ
 Brinkmann, W., Wang, T., Grupe, D., & Raeth, C. 2006, A&A, 450, 925
 Castor, J.I. 1972, ApJ, 178, 779
 Holt, J., Tadhunter, C., Morganti, R., Bellamy, M., González Delgado, R.M., Tzioumis A., & Inskip K.J. 2006, MNRAS, 370, 1633
 Icke, V. 1980, AJ, 85, 329
 King, A. R., & Pounds, K. A. 2003, MNRAS, 345, 657
 Mihalas, D. 1980, ApJ, 237, 574
 Nishiyama, S., Watarai, K., & Fukue, J. 2007, submitted to PASJ
 Ohsuga, K., Mori, M., Nakamoto, T., & Mineshige, S. 2005, ApJ, 628, 368
 Paczyński, B. 1990, ApJ, 363, 218
 Pounds, K.A., Reeves, J.N., King, A.R., Page, K.L., O'Brien, P.T., & Turner, M.J.L. 2003a, MNRAS, 345, 705
 Pounds, K.A., King, A.R., Page, K.L., & O'Brien, P.T. 2003b, MNRAS, 346, 1025
 Proga, D. 2003, ApJ, 585, 406
 Quinn, T., & Paczyński, B. 1985, ApJ, 289, 634
 Ruggles, C.L.N., & Bath, G.T. 1979, A&A, 80, 97
 Rybicki G.B., & Lightman A.P. 1979, *Radiative Processes in Astrophysics* (New York: John Wiley & Sons)
 Tajima, Y., & Fukue, J. 1998, PASJ, 48, 529
 Turolla, R., Nobili, L., & Calvani, M. 1986, ApJ, 303, 573
 Watarai, K., & Fukue, J. 1999, PASJ, 51, 725